

PROCEEDINGS OF SPIE

[SPIDigitalLibrary.org/conference-proceedings-of-spie](https://spiedigitallibrary.org/conference-proceedings-of-spie)

Processing and analysis of images in the multifunctional classification laser polarimetry system of biological objects

Zabolotna, Natalia, Pavlov, Sergei, Karas, Oleksandr, Sholota, Vladyslava

Natalia I. Zabolotna, Sergei V. Pavlov, Oleksandr V. Karas, Vladyslava V. Sholota, "Processing and analysis of images in the multifunctional classification laser polarimetry system of biological objects," Proc. SPIE 10750, Reflection, Scattering, and Diffraction from Surfaces VI, 107500N (4 September 2018); doi: 10.1117/12.2320209

SPIE.

Event: SPIE Optical Engineering + Applications, 2018, San Diego, California, United States

Processing and analysis of images in the multifunctional classification laser polarimetry system of biological objects

Natalia I. Zabolotna^a, Sergei V. Pavlov^a, Oleksandr V. Karas^a, Vladyslava V. Sholota^a

Vinnitsia National Technical University, 95 Khmelnytske Shose, Vinnitsia, Ukraine

ABSTRACT

The Jones matrix mapping of blood plasma films was considered in this paper. The statistical analysis (statistical moments of the 1st - 4th orders) of the obtained elements was carried out. To increase the accuracy and reliability of the diagnosis, the number of informative indicators was increased due to the correlation analysis, which increased the number of inputs to 8. The differentiation of nosologies was based on the rules of fuzzy logic.

Keywords: polarimetry, Jones-matrix, statistical analysis, correlational analysis.

1. INTRODUCTION

Methods of optical diagnostics on the basis of scattering of optical radiation by biological objects have been widely developed recently. The results obtained, for example, in the cycle of works¹⁻³ unambiguously indicate the promising use of polarimetric researches for developing new methods and approaches in the study of biological objects.

There is a large number of practical techniques based on measuring and analyzing the elements of the Jones matrix for objective analysis of the structure of the studied samples of different nature, in particular - biological⁴⁻⁶. Another group of methods widely used for the analysis and evaluation of biological objects are diagnostic methods based on classical polarimetry, Muller matrices, and Stokes-polarimetry. In particular, a method and an informative evaluation of the polarization mapping of azimuths and phase elements of the polarization of microscopic laser plasma films images for the diagnosis of benign and malignant changes in the mammary gland is proposed in work⁷.

Despite the existing methods for differentiation and diagnosis of the studied breast samples, it can be argued that they are not informationally complete, therefore, there is a need to extend the range of diagnostic criteria by introducing new methods for obtaining such criteria, in particular - at the expense of the Jones matrix method. The purpose of this work is to experiment with the investigation of optically thin human plasma layers by using the Jones matrix mapping of real elements of the Jones matrix, followed by statistical processing of the obtained maps to obtain new criteria for the differentiation of the studied samples.

The aim is to ensure the rapidity of the measurement and analysis of the obtained data and the reliability of the diagnostic methods. Required time operation characteristics of the specified system are provided by applying the principles of parallelism in the execution of basic image processing operations.

2. THE MULTIFUNCTIONAL CLASSIFICATION LASER POLARIMETRY SYSTEM

Multifunctional classification laser polarimetry system with the ability to implement twenty functions with different levels of information was developed: from measurement and analysis of distributions of Stokes parameters and Mueller-matrix elements of the investigated sample, to reproduction and analysis of orientational-phase parameters of anisotropy distribution of biological objects. The system consists of a measuring channel with the help of which new and improved methods of measurements of thin multilayer optical anisotropy biological object in the form of two-dimensional images were implemented, and the computer in which processing, analysis and classification of image data were realized (Fig. 1)⁸.

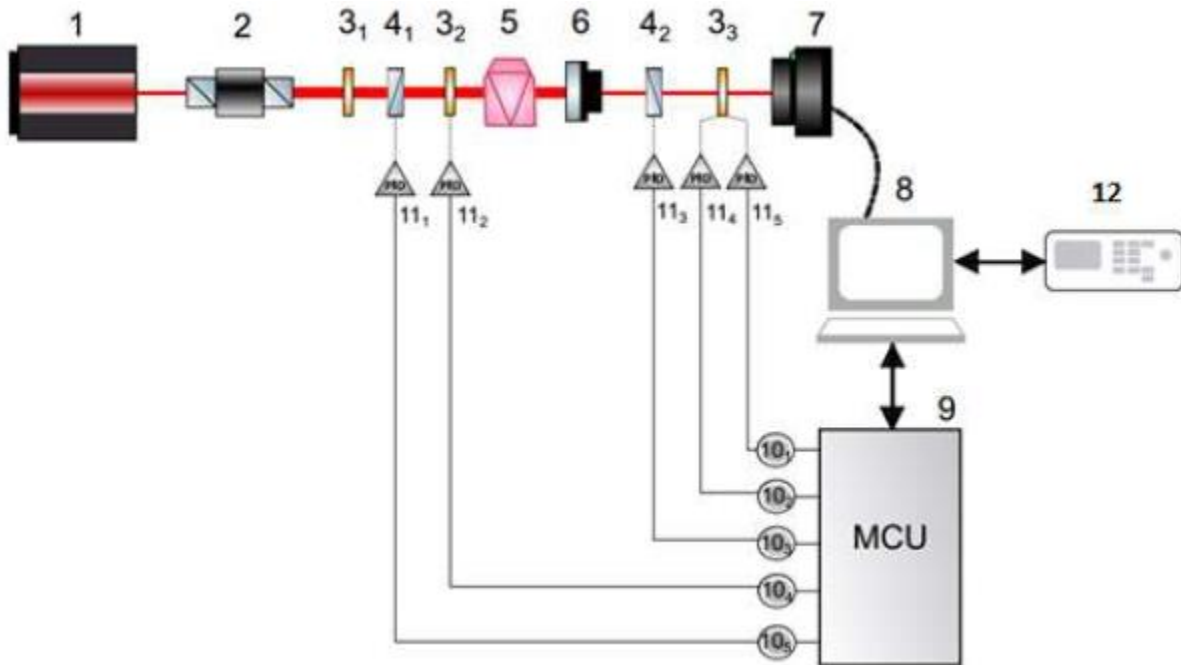


Figure 1. The multifunctional classification laser polarimetry system⁸

The system consists of a semiconductor laser 1 with $\lambda=0,638$ wavelength, collimator 2, quarter-wave plates 3₁, 3₂, 3₃, a linear polarizer 4₁ and an analyzer 4₂; blood plasma sample 5, projection block 6, a CCD-based (charge-coupled device) camera 7, connected to the computer 8; special microcontroller control block 9, engine drivers 10₁-10₅, positioning control of engines 11₁-11₅, decision support block 12. More details about the operation of this system are described in past works⁹⁻¹¹.

2.1 Principles of the system's work

To assess the presence of a pathological condition of the mammary gland, a sample of blood is taken and the plasma is isolated by means of a centrifuge. Blood plasma specimens were prepared under the following conditions: a drop of blood plasma was applied to a substrate of optically homogeneous glass so that the plasma spread evenly over the glass surface¹²⁻¹⁴.

The laser irradiation through an investigation sample of a plasma is carried out by a polarized coherent parallel beam ($10^4 \mu\text{m}$ in diameter) of a semiconductor laser ($\lambda = 0.6328 \mu\text{m}$) 1, which is formed by a collimator 2 and a quarter wave plate 3₁. Using the rotation of the polarizer 4₁ at the angles 0° - 90° , a linearly polarized beam with an azimuth $\alpha_0=0..90^\circ$

is formed, by which an anisotropic layer of biological object 5 is probing. By rotating the axis of the analyzer 4₂ in the range of 0°-90°, the image of the anisotropic layer of the biological object 5 is projected, using a micro-objective, in the plane of the photosensitive area (mxn = 640x480) of the digital camera 7, and then transmitted to the computer 8, and the array of levels of the intensity for each individual pixel is measured¹¹.

3. STATISTICAL AND CORRELATION ANALYSIS OF JONES MATRIX OF BLOOD PLASMA FILMS

To estimate the distributions $R_{ik}(X,Y)$ quantitatively their quantitative estimation is introduced on the basis of the definition of a set of their statistical moments of the 1st-4th order⁹⁻¹¹:

$$M_1 = \frac{1}{N} \sum_{j=1}^N (X_{ik})_j; M_2 = \sqrt{\frac{1}{N} \sum_{j=1}^N (X_{ik}^2)_j};$$

$$M_3 = \frac{1}{M_2^3} \frac{1}{N} \sum_{j=1}^N (X_{ik}^3)_j; M_4 = \frac{1}{M_2^4} \frac{1}{N} \sum_{j=1}^N (X_{ik}^4)_j. \quad (1)$$

The basis of the correlation approach is the method of autocorrelation analysis of Jones matrix images $R_{ik}(X,Y)$ ¹⁵ with the use of the autocorrelation function $G_{ik}(\Delta x, \Delta y)$ of the form:

$$G_{ik}(\Delta x, \Delta y) = \lim_{x,y \rightarrow \infty} \frac{1}{m \times n} \int_0^m \int_0^n [R_{ik}(x_{1+m}, y_{1+n})][R_{ik}(x - \Delta x, y - \Delta y)] dx dy, \quad (2)$$

where $(\Delta x, \Delta y)$ – "steps" with which the coordinates (x, y) of the distributions of the elements of the Jones matrix $R_{ik}(X,Y)$; m, n – numbers of pixels in the row and the column of the receiving plane of the camera.

In order to provide an objective comparative analysis of the autocorrelation dependencies of the Jones matrix elements of blood plasma films, we will conduct their statistical estimation:

$$K_1 = \frac{1}{N} \sum_{j=1}^N (\overline{R_{ik}}(\Delta x))_j; K_2 = \sqrt{\frac{1}{N} \sum_{j=1}^N (\overline{R_{ik}}(\Delta x)^2)_j};$$

$$K_3 = \frac{1}{M_2^3} \frac{1}{N} \sum_{j=1}^N (\overline{R_{ik}}(\Delta x)^3)_j; K_4 = \frac{1}{M_2^4} \frac{1}{N} \sum_{j=1}^N (\overline{R_{ik}}(\Delta x)^4)_j, \quad (3)$$

where $\overline{R_{ik}}(\Delta x)$ – the average approximation of the autocorrelation function in coordinate x .

4. RESULTS AND DISCUSSION

By sequentially fixing the change in the intensity of each pixel of the output laser beam, and by performing simple mathematical calculations, the elements of the Johns matrix of blood plasma films were obtained. In fig. 2 shows samples of polarimetric mappings of the Jones matrix elements of blood plasma films.

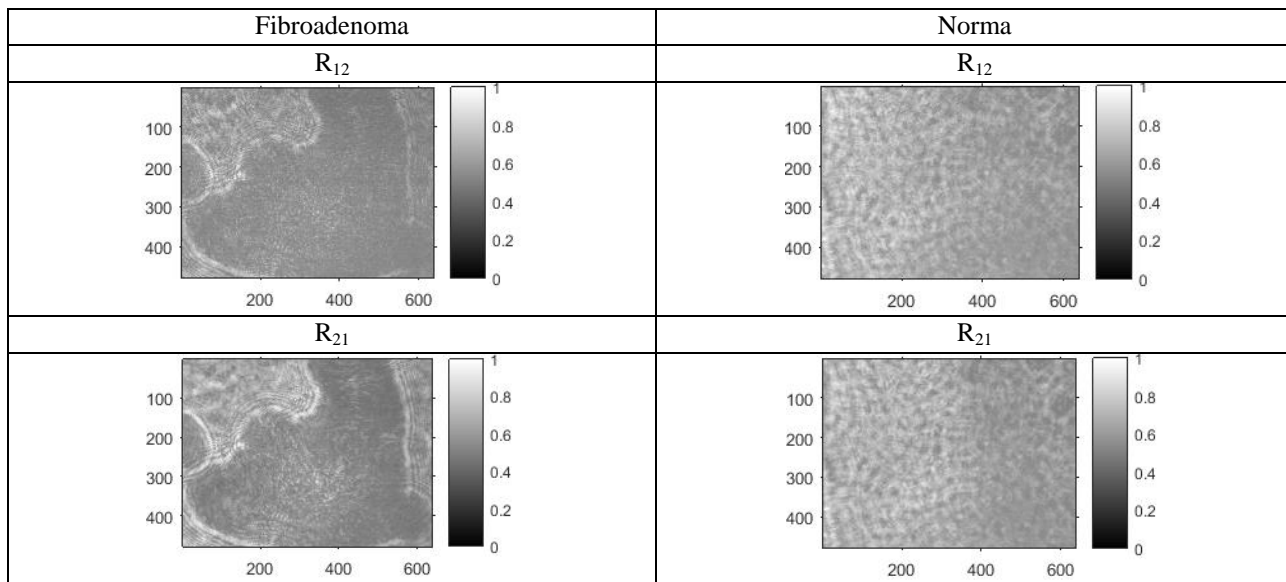


Figure 2. Images of polarizationally reproduced elements (real component of Jones-matrix) of a blood plasma with nosologies: fibroadenoma and norm.

In order to objectively evaluate the statistical dependencies between the norm nosologies and fibroadenoma, a calculation of four statistical moments (mean, variance, asymmetry and excess) was performed.

To improve the accuracy of the measurements, a correlation analysis of the actual elements of the Jones matrix of blood plasma films was performed. Figure 3 shows the input image of the R_{12} Jones matrix element of blood plasma film, the significance of the statistical moments of the 1st to the 4th orders, the actual autocorrelation function calculated with the one-dimensional approximation for the coordinate x , and the histogram for determining the coordinate distribution of the Jones matrix elements.

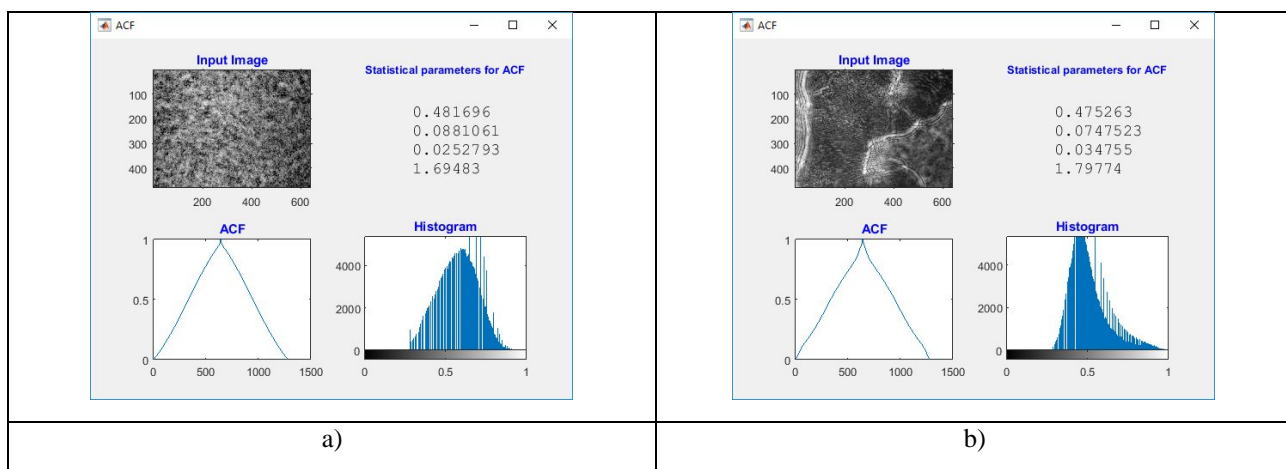


Figure 3. Input image, statistical parameters for autocorrelation function (ACF), ACF and histogram of: a) Jones-matrix elements with nosology Norm; b) Jones-matrix elements with nosology Fibroadenoma

In order to objectively and quantitatively characterize the difference in the distribution of the autocorrelation function for different nosologies, a calculation of statistical characteristics was carried out using formulas 3. Tables 1, 2 show the statistical and correlation distribution of the actual elements of the Jones matrix of blood plasma films for nosologies - norm and fibroadenoma.

Table 1. Average (M_1, K_1), variance (M_2, K_2), asymmetry (M_3, K_3) and excess (M_4, K_4) of distributions of elements of the Jones-matrix (real component) and autocorrelation function of blood plasma films polarization images for nosology – norm.

Norm	R_{11}	R_{21}	R_{12}	R_{22}
M_1	$0,76 \pm 0,019$	$0,67 \pm 0,075$	$0,72 \pm 0,067$	$0,96 \pm 0,034$
M_2	$0,015 \pm 0,003$	$0,0077 \pm 0,0064$	$0,0054 \pm 0,0038$	$0,0048 \pm 0,0034$
M_3	$-0,32 \pm 0,16$	$0,33 \pm 0,53$	$0,2 \pm 0,41$	$-3,99 \pm 2,79$
M_4	$2,79 \pm 0,44$	$3,63 \pm 1,0$	$2,78 \pm 0,35$	$34,14 \pm 30,34$
K_1	$0,49 \pm 0,005$	$0,495 \pm 0,005$	$0,49 \pm 0,01$	$0,5 \pm 0,005$
K_2	$0,0845 \pm 0,0015$	$0,085 \pm 0,002$	$0,084 \pm 0,004$	$0,0845 \pm 0,0005$
K_3	$0,028 \pm 0,019$	$0,014 \pm 0,011$	$0,0135 \pm 0,0115$	$0,00466 \pm 0,00464$
K_4	$1,76 \pm 0,001$	$1,275 \pm 0,33$	$1,76 \pm 0,07$	$1,785 \pm 0,015$

Table 2. Average (M_1, K_1), variance (M_2, K_2), asymmetry (M_3, K_3) and excess (M_4, K_4) of distributions of elements of the Jones-matrix (real component) and autocorrelation function of blood plasma films polarization images for nosology – fibroadenoma.

Fibroadenoma	R_{11}	R_{21}	R_{12}	R_{22}
M_1	$0,76 \pm 0,01$	$0,53 \pm 0,044$	$0,57 \pm 0,033$	$0,9 \pm 0,06$
M_2	$0,021 \pm 0,0034$	$0,019 \pm 0,015$	$0,01 \pm 0,006$	$0,01 \pm 0,005$
M_3	$-0,21 \pm 0,45$	$0,56 \pm 0,73$	$1,03 \pm 0,78$	$-1,28 \pm 0,79$
M_4	$2,57 \pm 0,53$	$3,77 \pm 1,58$	$4,83 \pm 2,167$	$4,65 \pm 2,19$
K_1	$0,485 \pm 0,005$	$0,485 \pm 0,005$	$0,465 \pm 0,025$	$0,495 \pm 0,005$
K_2	$0,082 \pm 0,003$	$0,081 \pm 0,002$	$0,078 \pm 0,004$	$0,0825 \pm 0,0025$
K_3	$0,034 \pm 0,014$	$0,036 \pm 0,029$	$0,072 \pm 0,059$	$0,00985 \pm 0,00415$
K_4	$1,755 \pm 0,025$	$1,78 \pm 0,02$	$1,795 \pm 0,015$	$1,7759 \pm 0,0059$

In order to determine how informative this or that indicator was, circular diagrams of the value of intervals of ranges of changes in the values of a set of statistical and correlation characteristics were constructed. Examples of some of them are shown in Fig. 4.

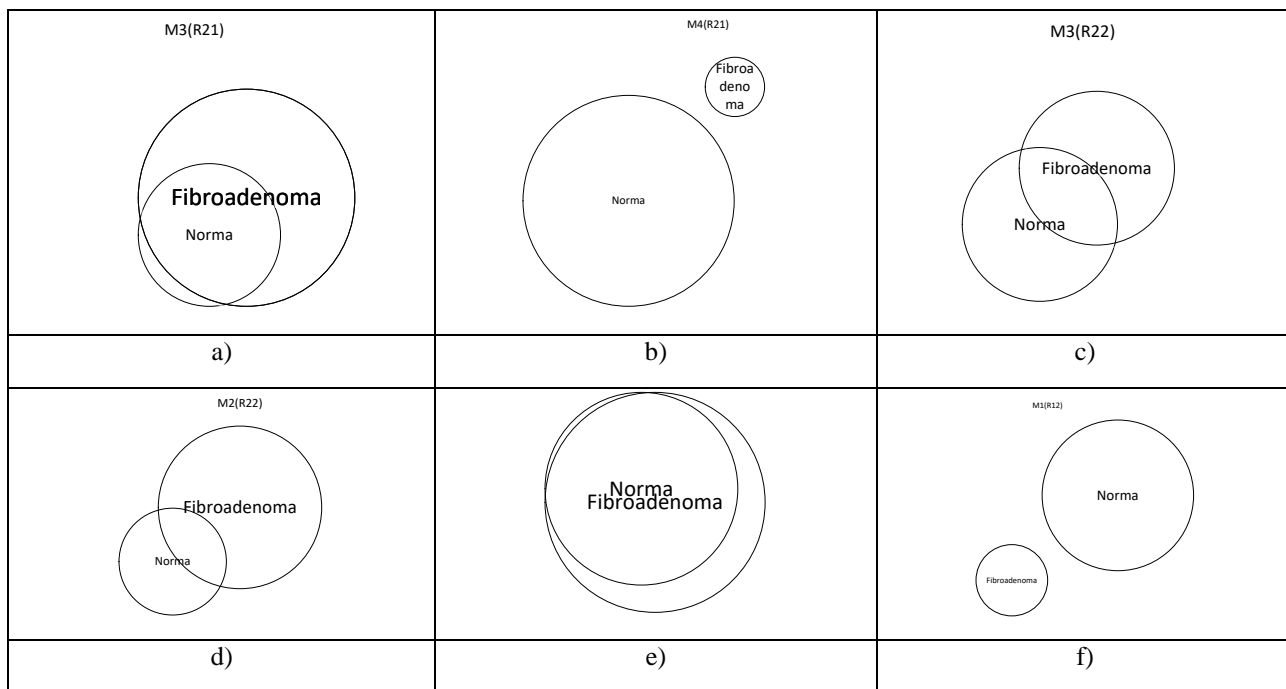


Figure 4 Statistical and correlation distribution of the values of the elements of the Jones matrix of blood plasma films; b, f – fully informative indicators; c, d – partially informative indicators; a, e – non-informative indicators.

As a result of the analysis, it was found that the most informationally sensitive statistical analysis are the 1st [$M_1(R_{12})$] and the 2nd statistical points [$M_2(R_{11}, R_{21}, R_{12}, R_{22})$]; according to the correlation analysis, the most informative were the 3rd [$M_3(R_{21}, R_{12}, R_{22})$] and the 4th [$M_4(R_{21})$] correlation moments.

The next step is the differentiation of nosologies with the help of a decision support system based on the rules of fuzzy logic¹⁶. For this purpose, a database based on the values of informative indicators was created and membership functions were constructed for statistical and correlation analysis of the Jones matrix elements of plasma blood films (Figure 5).

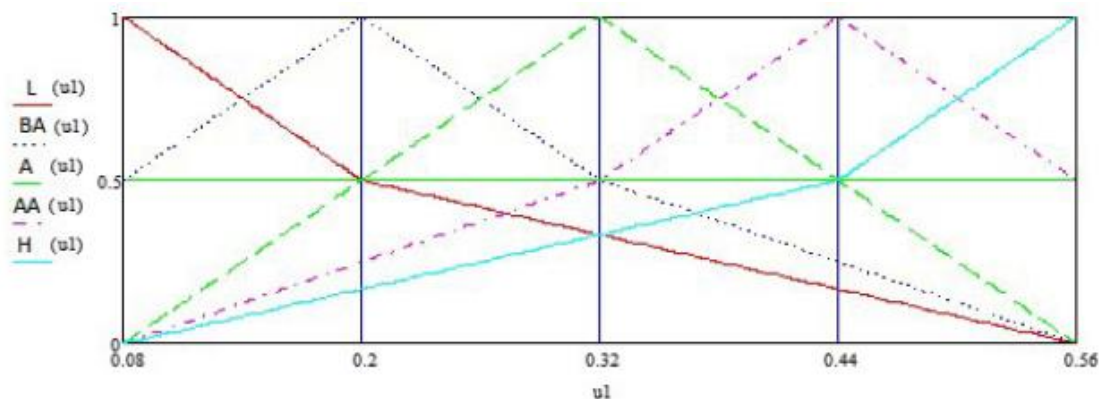


Figure 5. View of membership functions for statistical and correlation moments of the Jones-matrix real component

5. CONCLUSIONS

Multifunctional classification laser polarimetry system was developed. The statistical and correlation analysis of the Jones matrix elements was carried out. As a result of the analysis, it was found that the most informationally sensitive statistical analysis are the 1st [$M_1(R_{12})$] and the 2nd statistical points [$M_2(R_{11}, R_{21}, R_{12}, R_{22})$]; according to the correlation analysis, the most informative were the 3rd [$M_3(R_{21}, R_{12}, R_{22})$] and the 4th [$M_4(R_{21})$] correlation moments. The differentiation of nosologies was based on the rules of fuzzy logic.

REFERENCES

- [1] Tuchin V. V. Optical Polarization in Biomedical Applications / Tuchin V. V., Wang L. V., Zimnyakov D. A. — Berlin : Springer, 2006. — 285 p.
- [2] Wang X. Monte Carlo model and single-scattering approximation of polarized light propagation in turbid media containing glucose / X. Wang, G. Yao, L. - H. Wang // *Appl. Opt.* – 2002. – Vol. 41. – P. 792-801.
- [3] Shuliang J. Two-dimensional depth-resolved Mueller matrix of biological tissue measured with double-beam polarization-sensitive optical coherence tomography / J. Shuliang, V. W. Lihong // *Opt. Lett.* – 2002. – Vol. 27. – P. 101-103.
- [4] Shuichi Makita, Kazuhiro Kurokawa, Young-Joo Hong, Masahiro Miura, and Yoshiaki Yasuno, «Noise-immune complex correlation for optical coherence angiography based on standard and Jones matrix optical coherence tomography» *Biomed. Opt. Express* 7, 1525—1548 (2016).
- [5] Yoshiaki Yasuno, Shuichi Makita, Takashi Endo, Masahide Itoh, Toyohiko Yatagai, Mari Takahashi, Chikatoshi Katada and Manabu Mutoh, «Polarization-sensitive complex Fourier domain optical coherence tomography for Jones matrix imaging of biological samples,» *Appl. Phys. Lett.* 85, 3023—3025 (2004).
- [6] Jiao S , Wang L V; Jones-matrix imaging of biological tissues with quadruple-channel optical coherence tomography. *J. Biomed. Opt.* 0001;7(3): 350—358.
- [7] Natalia I. Zabolotna, Bogdan P. Oliinychenko, Kostiantyn O. Radchenko, Anastasiia K. Krasnoshchoka, Olga K. Shcherba, «System of polarization phasometry of polycrystalline blood plasma networks in mammary gland pathology diagnostics», in *Polarization Science and Remote Sensing VII*, Daniel A. LeMaster; Joseph A. Shaw, Editors, *Proceedings of SPIE Vol. 9613* (SPIE, Bellingham, WA 2015), 961311.
- [8] Natalia I. Zabolotna, Kostiantyn O. Radchenko, Oleksandr V. Karas, "Method and system of Jones-matrix mapping of blood plasma films with “fuzzy” analysis in differentiation of breast pathology changes", *Proc. SPIE 10612*, Thirteenth International Conference on Correlation Optics, 106121P (18 January 2018).
- [9] Natalia I. Zabolotna, Sergii V. Pavlov, Kostiantyn O. Radchenko, Vladyslav A. Stasenko, Waldemar Wójcik, Nazym Kussambayeva “Diagnostic efficiency of Mueller - matrix polarization reconstruction system of the phase structure of liver tissue” *Proc. SPIE 9816*, *Optical Fibers and Their Applications*, 98161E (2015).
- [10] Natalia I. Zabolotna, Kostiantyn O. Radchenko “A multifunctional automated system of 2D laser polarimetry of biological tissues,” *Proc. SPIE 9205*, *Reflection, Scattering, and Diffraction from Surfaces*, 92050V (2014).

- [11] Natalia I. Zabolotna, Kostiantyn O. Radchenko, Mykola H. Tarnovskiy, "System of Mueller-Jones matrix polarizing mapping of blood plasma films in breast pathology," Proc. SPIE 10407, Polarization Science and Remote Sensing VIII, 1040714 (2017).
- [12] P. Mintser, N. I. Zabolotna, B. P. Oliinychenko and P. Komada "Differential phase analysis of laser images of a polycrystalline component of blood plasma in diagnostics of pathological changes in mammary gland," Proc. SPIE 8698, Optical Fibers and Their Applications, 86980D (2013).
- [13] Ushenko Yu. A., Ushenko V.A., Dubolazov A.V., Balanetskaya V.O, Zabolotna N.I. "Mueller–matrix diagnostics of optical properties of polycrystalline networks of human blood plasma," Optics and Spectroscopy, 112(6), 884–892 (2012).
- [14] N.I. Zabolotna , B.P. Oliinychenko, K.O. Radchenko, Krasnoshchoka A.K. and Shcherba O.K. "System of polarization phasometry of polycrystalline blood plasma networks in mammary gland pathology diagnostics," Proc. SPIE. 9613, Polarization Science and Remote Sensing, 961311 (2015).
- [15] Ushenko Ye.G. Correlation Structure of Mueller Matrices of Biotissues and their Physiological State Diagnostics / Ye.G. Ushenko, Yu.A. Ushenko, O.I . Olar, V.P. Pishak, O.V. Pishak // 5th International Conference "Mechatronics-2004". Warshava, 2004. – P. 315-317.
- [16] Lotfi A. Zadeh, "Fuzzy logic: principles, applications, and perspectives," Proc. SPIE 1468, Applications of Artificial Intelligence IX, (1 March 1991).